A TWO-STEP IMAGING PROCEDURE FOR MEG CHARACTERIZATION OF CORTICAL CURRENTS: LOCATION AND SPATIAL EXTENT.

S. Khan [1,2], *B. Cottereau* [1,3], *R. M. Leahy*[4], *J. C. Mosher*[5], *H. Ammari*[6], *S. Baillet*[1,2]

[1] Cognitive Neuroscience & Brain Imaging Laboratory
CNRS; Hôpital de la Salpêtrière, Paris, France
[2] UPMC Univ Paris 06
[3] ESME-Sudria College of Engineering, Ivry, France
[4] University of Southern California, Los Angeles, USA
[5] Los Alamos National Laboratory, USA
[6] Laboratoire Ondes et Acoustique, CNRS & ESPCI, Paris, France

ABSTRACT

There is theoretical and experimental evidence that the spatial extent of mass neural activity is an important factor of brain response in neuroimaging studies. Direct estimation of the surface area of activated regions would importantly complement the quantitative analysis of amplitude variations of cortical currents. These latter are accessible at the regional scale through source modeling of magnetoencephalographic signals. Here we present a joint approach to the estimation of both the local spatial extent and amplitude variations of neural current sources. The technique operates in two consecutive steps: 1) the compact modeling of regional cortical currents using equivalent current multipoles and 2) the remapping of these latter back onto the cortical surface using a sparse-focal imaging model. This Multipole Cortical Remapping technique operates in a Bayesian framework. Performances are evaluated using extensive Monte-Carlo simulations and are complemented with real data from a somatosensory mapping MEG experiment.

Index Terms— Electromagnetic brain imaging, magnetoencephalography (MEG), current multipoles.

1. INTRODUCTION

Electromagnetic brain imaging techniques using electro and magnetoencephalography (EEG and MEG, respectively) have considerably matured in terms of detecting variations of neural current amplitudes at the cortical level (see [1] for a recent illustration). Variations of loco-regional surface/volume extent of brain activity is another element of stimulus-induced brain responses that has seldom ever been considered from a methodological imaging viewpoint so far. There are hypotheses however that this parameter would be relevant to multiple and crucial neuroscience questions such as plasticity of neural assemblies for instance [2].

To approach the estimation of the surface extent of neural responses at the regional scale would require that an imaging model with sparse-focal priors be fitted to the measurements. MEG/EEG literature has been extensively reporting on such approaches (see e.g. [3] for a recent reference) but these latter have revealed behaving poorly in the experimental practice, principally because of numerical limitations. Parametric models such as the equivalent current dipole (ECD) – though respecting the expectancy of spatial sparsity – carries no explicit information about the spatial extent of the generating currents, which are cortically-distributed by nature.

To address these difficulties we introduce a new procedure – called Multipole Cortical Remapping (MCR) – which takes advantage of both the compact parametric modeling of distributed currents using equivalent current multipoles (ECM) and sparse-focal image models on restricted spatial supports – yields a workable estimation of the surface extent of regional brain activations. The MCR proceeds as follows: first, parametric modeling of cortical currents is obtained by fitting a series of compact equivalent current multipole (ECM) model elements to a low-resolution regularized image of the cortically-constrained current distribution. The second step consists in efficiently adjusting a sparse-focal image model to each ECM element using a maximum a posteriori (MAP) Bayesian estimation framework. Hence the ECM decomposition acts an intermediary between two image models of cortical currents, for the sake of considerable reduction in the dimensions of the parameter subspaces.

2. MULTIPOLE CORTICAL REMAPPING

2.1. Compact parametric decomposition of cortical currents

The motivation is to reduce the dimension of the subspace in which a sparse focal image model may be fitted to the data.

One approach could consist in directly adjusting equivalent current dipole (ECD) or ECM models to the data. The non-linear search for their optimal locations though has proven to be hardly tractable in practice without strong priors on the number and the expected loci of activations when multiple regions are simultaneously active.

Here the decomposition of cortical currents in a compact form using ECM model elements relays a smooth, low-resolution image model of neural currents to their final higher-resolution sparse-focal estimate in a two-step procedure.

The basic image support consists of a set $\mathcal{D}$ of n elementary current dipoles $\mathcal{D} = \{\mathbf{d}_i, i \leq n\}$, densely distributed over the MRI-extracted cortex of the subject that forms a surface manifold Γ of $\mathbb{R}^3$. The orientations $\mathbf{o}_i$ of all dipoles follow the circumvolutions of the cortical mantle. Hence the estimation of cortical currents reduces to that of their amplitude distribution $\mathbf{y} = \{y_i, i \leq n\}$.

The low-resolution image model was obtained from the Tikhonov-regularized weighted minimum-norm estimator (WMNE)[4]:

$$\overline{\mathbf{y}} = \arg\min_{\mathbf{y}}\{\|\mathbf{b} - \mathbf{Gy}\|^2 + \lambda\mathbf{y}^{\mathbf{t}}\mathbf{C}^{-1}\mathbf{y}\}, \qquad (1)$$

where $\mathbf{b}$ is a vector of m instantaneous measurements on the MEG sensor array; $\mathbf{G}$ is the corresponding forward gain matrix and $\mathbf{C}$ is the expected covariance matrix of the elementary sources; λ is a scalar regularization parameter. The solution to (1) is unique and takes the following form:

$$\overline{\mathbf{y}} = \mathbf{G}^{\mathbf{t}}(\mathbf{GG}^{\mathbf{t}} + \lambda\mathbf{I})^{-1}\mathbf{b}, \qquad (2)$$

where $\mathbf{G}^{\mathbf{t}}$ denotes the transposed $\mathbf{G}$ matrix and we have assumed $\mathbf{C} = \mathbf{I}$ without loss in generality. Note that $\overline{\mathbf{y}}$ may either be estimated at a single time instant or over a larger time frame with no difference in the approach.

The low-resolution image model $\overline{\mathbf{y}}$ was thresholded using e.g. an absolute amplitude criterion based on the analysis of the histogram of the $|y_i|$'s. Dipole elements in $\mathcal{D}$ with absolute amplitude under the 85th percentile of the histogram were set to zero. The remaining set of *active* elementary dipoles was arranged in a set of n_C spatially-contiguous dipole clusters $\{\mathcal{C}_j, j \leq n_C\}$ [5]. Let $\mathbf{x_i}$ be the coordinates of dipole $\mathbf{d}_i$ in $\mathbb{R}^3$. We define as $\mathbf{X}_j$, the current-weighted centroid of cluster $\mathcal{C}_j$, that is:

$$\mathbf{X}_j = \sum_{i,\mathbf{d}_i \subset \mathcal{C}_j} |y_i|\mathbf{x}_i.$$

$\mathbf{X}_j$ serves as the expansion point of the ECM model $\mathbf{m}_{\mathcal{C}_j}$ – up to the quadrupole – of the currents sustained by cluster $\mathcal{C}_j$. All the ECM moments from all clusters are gathered in $\mathbf{m}_{\mathcal{C}}$ and are adjusted in the least-squares sense:

$$\mathbf{m}_{\mathcal{C}} = \mathbf{G}_{\mathbf{m}}^{\mathbf{t}}(\mathbf{G}_{\mathbf{m}}\mathbf{G}_{\mathbf{m}}^{\mathbf{t}})^{-1}\mathbf{b}, \qquad (3)$$

where $\mathbf{G}_{\mathbf{m}}$ is the ECM gain matrix of all the $\mathcal{C}_j$ ($j \leq n_c$) clusters, which computation is detailed in [6].

2.2. Sparse-focal imaging model

The second step in the MCR procedure consists of estimating an equivalent cortical current distribution to each of the ECM elements $\mathbf{m}_{\mathcal{C}_j}$ using explicit sparse-focal priors.

The quadrupolar ECM expansion $\mathbf{m_i} \in \mathbb{R}^7$ of any dipole $\mathbf{d}_i \subset \mathcal{C}_j$ about $\mathbf{X}_j = [X_{j,1}, X_{j,2}, X_{j,3}] \in \mathbb{R}^3$, writes [7]:

$$\mathbf{m_i} = \begin{bmatrix} 1 & 0 & 0 \\ 0 & 1 & 0 \\ -X_{j,1} & -X_{j,2} & 2X_{j,3} \\ X_{j,3} & 1 & X_{j,1} \\ 0 & X_{j,3} & X_{j,2} \\ .5X_{j,1} & -.5X_{j,2} & 0 \\ .5X_{j,2} & .5X_{j,1} & 0 \end{bmatrix} \mathbf{o_i} \cdot y_i = \mathbf{g_i^m}y_i. \quad (4)$$

The equivalent sparse-focal image model of each $\mathbf{m}_{\mathcal{C}_j}$ defined in section 2.1 consists of a subset of cortical dipoles $\zeta_j \subset \mathcal{D}$ which amplitudes $\overline{\overline{\mathbf{y}}}_j$ verify:

$$\mathbf{m}_{\mathcal{C}_j} = \sum_{i,\mathbf{d}_i \in \zeta_j} \mathbf{g_i^m}\overline{\overline{y}}_i + \mathbf{n} = \mathbf{G}_j^m\overline{\overline{\mathbf{y}}}_j + \mathbf{n}, \qquad (5)$$

where $\mathbf{n}$ is the residuals between the ECM element $\mathbf{m}_{\mathcal{C}_j}$ and its cortically-distributed counterpart. $\overline{\overline{\mathbf{y}}}$ is estimated using explicit sparse-focal priors, which can readily be inscribed in a Bayesian MAP estimator of cortical current amplitudes exemplified in [8]. This has been demonstrated e.g. in the context of Markovian Random Field (MRF) models of the cortical current distribution. Here, we revisit this approach and make it tractable by running MAP estimates restricted to the local current distributions about each ECM element and by matching their respective multipolar moments. The cortical current density is modeled as a random process using extensions of the models described in [8]. We characterize the current density $\overline{\overline{y}}_i$ at every vertex through the association of a continuous, normally-distributed, random variable of dipole amplitude z_i and a binary indicator process x_i of whether source i is on or off. Thus $\overline{\overline{y}}_i = x_i z_i$, and globally $\overline{\overline{\mathbf{y}}} = \mathbf{x} * \mathbf{z}$, with $\mathbf{x}$ and $\mathbf{z}$ assumed being two independent processes.

The MAP estimate of the set of dipole amplitudes that will match the ECM moments of $\mathbf{m}_{\mathcal{C}_j}$ writes:

$$\overline{\overline{\mathbf{y}}}_j = \{x_i z_i, \mathbf{d}_i \in \zeta_j\} = \arg\max_{\mathbf{x}, \mathbf{z}} p(\mathbf{x}, \mathbf{z}|\mathbf{m_{C_j}}). \qquad (6)$$

The underlying MRF of the indicator process $\mathbf{x}$ follows a Gibbs distribution which energy function $V(x)$ writes:

$$V(\mathbf{x}) = \sum_{i,\mathbf{d}_i \in \zeta_j} (\alpha_i x_i + \beta_i \sum_{k \in \nu^i} \frac{(x_i - x_k)^2}{\gamma_{ik}}), \qquad (7)$$

where $\alpha_i > 0$ and $\beta_i > 0$ determine the sparseness and clustering relative weights; ν^i is the set of nearest neighbors of vertex i, and γ_{ik} is proportional to the geodesic distance between $\mathbf{d}_i$ and $\mathbf{d}_k$ and to the discrepancy between their orientations.

Source amplitudes $\mathbf{z}$ are assumed to be centered and normally-distributed with covariance $\mathbf{C_z}$. Assuming the perturbation process in (5) to be zero-mean Gaussian with covariance matrix $\mathbf{C_n}$, the MAP estimation from (6) reduces to the minimization of the energy functional associated to the posterior distribution of $\overline{\overline{\mathbf{y}}}_j$:

$$U(\mathbf{x}, \mathbf{z}|\mathbf{m}_{\mathcal{C}_j}) = \frac{1}{2}[\mathbf{m}_{\mathcal{C}_j} - \mathbf{G}_j^m \mathbf{x} * \mathbf{z}]^t \mathbf{C}_n^{-1}[\mathbf{m}_{\mathcal{C}_j} - \mathbf{G}_j^m \mathbf{x} * \mathbf{z}]$$
$$+ \frac{1}{2}\mathbf{z}^\mathbf{T}\mathbf{C_z}^{-1}\mathbf{z} + V(x). \quad (8)$$

Identifying the elements of ζ_j is achieved through a recursive and iterative surfacic region-growing process. The process is recursive and it considers each dipolar source in $\mathcal{C}_j$ as a seed to a patch growing process. This latter consists of a recursive estimation of the local current density on a growing number of source candidates in the vicinity of every seed until $U(\mathbf{x}, \mathbf{z}|\mathbf{m}_{\mathcal{C}_j})$ is minimized. At each iteration, this latter is minimized with the iterated conditional mode (ICM) optimization of the binary indicator process.

For every seed $\mathbf{d}_i \in \mathcal{C}_j$:

1. Initialization: set $k = 1$, the patch around source i to $\nu_k^i = \{i\}$ and $U_0^i = 0$;

2. Estimate $\overline{\overline{\mathbf{y}}}_j$ and compute U_k^i from Eq. ;

3. If $|U_k^i - U_{k-1}^i| > \epsilon U_{k-1}^i$

   (a) Grow the patch by including the vertices connected to the source(s) in $\nu_k^i = \{i\}$;

   (b) Set k=k+1 and move to next seed in $\mathcal{C}_j$.

4. else:

   (a) Define $U^i = U_k^i$;

   (b) Define the best patch obtained from seed i, $\Pi^i = \nu_i^{k-1}$;

   (c) Proceed to next seed.

We define the optimal sparse focal equivalent image support to $\mathbf{m}_{\mathcal{C}_j}$ as:

$$\zeta_j = \cup_{i \in I} \Pi^i, \quad (9)$$

with

$$I = \{i, U^i \geq \overline{U}^i - 3\sigma_{U^i}\}, \quad (10)$$

where $\overline{U}^i$ (resp. σ_{U^i}) is the sample mean (resp. standard deviation) of the U^i's obtained for each seed at step 4a. This process is repeated for the n_c clusters.

3. RESULTS

3.1. Simulated data

We have challenged the MCR approach using Monte-Carlo (MC) simulations by growing 2,500 cortical patches with surface extents ranging from 5 to 30cm^2 on a high-resolution tessellation (37,723 vertices, 76,952 faces; 2.6mm^2 average triangle area) of the grey/white matter envelope obtained from the segmentation of a T1-weighted MR image series using the BrainSuite software (http://neuroimage.usc.edu/brainsuite). Uniform activation was assigned to the elementary cortical dipoles within a patch using a 100-time-sample Hamming waveform for active dipoles. The corresponding MEG signals were simulated on the CTF/VSMMedtech 151-axial gradiometers system using a spherical head model (Brainstorm software,http://neuroimage.usc.edu/brainstorm). Gaussian white noise was added with a uniform level across all the channels of 10% of the peak of maximum amplitude of the signal.

The model parameters were set to $\mathbf{C_n} = 10^{-2} \cdot \mathbf{I}$, $\mathbf{C_z} = 100 \cdot \mathbf{I}$, $\alpha_i = \beta_i = 10^{-5}$, $\gamma_{i,k} = 1$, $\epsilon = 10^{-6}$ and λ was estimated using the l-curve criterion.

An accuracy measure was defined as the normalized equally weighted sum of i) the distance between the original and remapped patch centroids, ii) the difference between the area of the original and remapped surface patches and iii) the subspace correlation between the forward fields of the original and remapped patches. This performance evaluating criteria takes it value from 0 (no match) and 1 (perfect match). Fig.1. shows that the performances of MCR are stable across the entire range of surface extents explored. The recovery of the
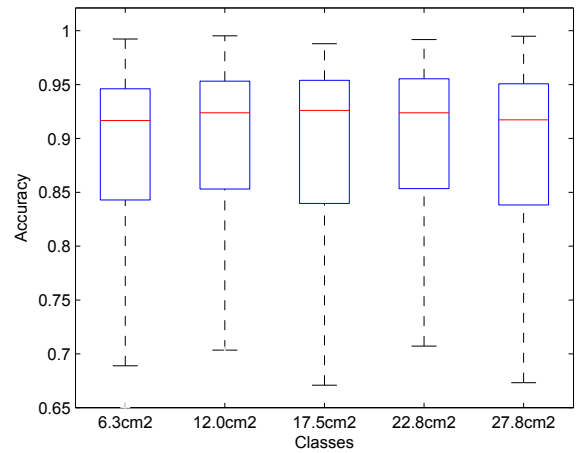

Fig. 1. Accuracy of MCR across multiple surface extents of activated areas; clustered into 5 classes (2,500 MC trials, 500 for each class). The boxplot indicates the lower quartile, median, and upper quartile values of each class and further, the entire span of the data.

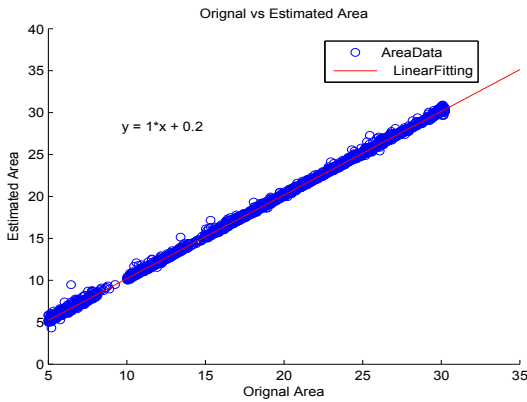original surface extent is further illustrated Fig.2.

Fig. 2. Original vs. estimated surface extent of activated areas (2,500 individual activated regions). The MCR estimator succeeds in recovering quantitatively the area of the original surface. Linear regression analysis indicates a correlation coefficient of 0.98 with an average error of 0.2 cm^2.

3.2. Application to real somatosensory data

We used a dataset from an MEG experiment that consisted in mapping the primary somatosensory response to stimulations of the hand fingers [9]. The stimulus consisted of an electrical square-wave pulse delivered separately to four fingers of each hand: thumb, index, middle, and pinky fingers. The magnetic fields were recorded with a 151 channel CTF/VSMMedtech MEG system. The trial duration was 300-ms long that included a 50-ms prestimulus interval; sampling rate was 1250 Hz. The MCR analysis of this data focussed of the early cortical response occurring about 40ms after stimulus delivery. Results revealed the expected somatotopic organization of the finger responses in the post-central SI area as shown Fig.3, with some overlap as expected from similar experiments on animal models. Table.1. contains the estimated surface areas of active cortex in response to stimulation.

Finger	Area (cm^2)	Finger	Area (cm^2)
Thumb	9.3	Index	3.6
Middle	5.2	Pinky	4.7

Table.1. Estimated areas of the cortical area activated by stimulation of the right hand fingers.

4. CONCLUSION

We have presented a fast (about 20 sec for a 37,723 node cortical tessellation) and promising method to localize and estimate the spatial extent of activated cortical regions in MEG. Further developments will consist of evaluating and correlating these new quantitative indices under various protocols and conditions.
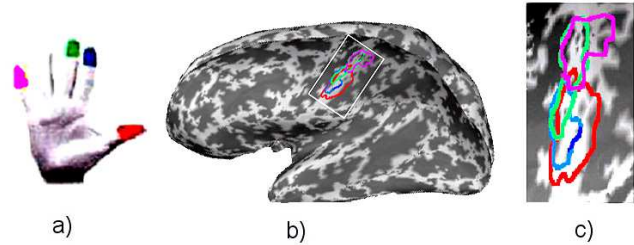

Fig. 3. Rendering of the estimated surfaces activated 40 ms after stimulus delivery. (a) Color code of the four fingers stimulated in the study; (b) The MCR estimates of the respective cortical responses.(c) Close-up view.

5. REFERENCES

[1] K. Jerbi, J.P. Lachaux, K. NDiaye, D. Pantazis, R.M. Leahy, L. Garnero, and S. Baillet, "Coherent neural representation of hand speed in humans revealed by MEG imaging," *Proc Natl Acad Sci U S A*, vol. 104, no. 18, pp. 7676–7681, May 2007.

[2] D. V. Buonomano and M. M. Merzenich, "Cortical plasticity: From synapses to maps," *Annual Review Of Neuroscience*, vol. 21, pp. 149–186, 1998.

[3] J. Daunizeau, J. Mattout, D. Clonda, B. Goulard, H. Benali, and J.M. Lina, "Bayesian spatio-temporal approach for eeg source reconstruction: conciliating ecd and distributed models.," *IEEE Trans Biomed Eng*, vol. 53, no. 3, pp. 503–516, Mar 2006.

[4] Clifford Thurber Richard Aster, Brian Borchers, Ed., *Parameter Estimation and Inverse Problems*, Academic Press, 2006.

[5] Robert M. Haralock and Linda G. Shapiro, *Computer and Robot Vision*, Addison-Wesley Longman Publishing Co., Inc., Boston, MA, USA, 1991.

[6] K. Jerbi, J.C. Mosher, Sylvain Baillet, and R.M. Leahy, "On meg forward modelling using multipolar expansions.," *Phys Med Biol*, vol. 47, no. 4, pp. 523–555, Feb 2002.

[7] J.P. Wikswo Jr and K.R. Swinney, "Scalar multipole expansions and their dipole equivalents," *Journal of Applied Physics*, vol. 57, pp. 4301, 1985.

[8] J. Phillips, J.C. Leahy, R.M.and Mosher, and B. Timsari, "Imaging neural activity using meg and eeg," *IEEE Eng. Med. Biol. Mag.*, vol. 16(3), pp. 34–42, 1997.

[9] S. Meunier, L. Garnero, and M. Vidailhet, "Human brain mapping in dystonia reveals both endophenotypic traits and adaptive reorganization," *Annals of Neurology*, vol. 50, no. 4, pp. 521–527, 2001.